A comparison of the field emission characteristics of vertically aligned graphene sheets grown on different SiC substrates*

Chen Lian-Lian(陈莲莲), Guo Li-Wei(郭丽伟)†, Liu Yu(刘 宇), Li Zhi-Lin(李治林), Huang Jiao(黄 郊), and Lu Wei(芦 伟)

Research & Development Center for Functional Crystals, Beijing National Laboratory for Condensed Matter Physics, Institute of Physics, Chinese Academy of Sciences, Beijing 100190, *China*

(Received 9 April 2012; revised manuscript received 6 May 2013)

The field emission (FE) properties of vertically aligned graphene sheets (VAGSs) grown on different SiC substrates are reported. The VAGSs grown on nonpolar SiC (10-10) substrate show an ordered alignment with the graphene basal plane-parallel to each other, and show better FE features, with a lower turn-on field and a larger field enhancement factor. The VAGSs grown on polar SiC (000-1) substrate reveal a random petaloid-shaped arrangement and stable current emission over 8 hours with a maximum emission current fluctuation of only 4%. The reasons behind the differing FE characteristics of the VAGSs on different SiC substrates are analyzed and discussed.

Keywords: field emission, vertically aligned graphene sheets, SiC substrate

PACS: 79.70.+q, 61.48.Gh **DOI:** 10.1088/1674-1056/22/10/107901

Conventional cathodes in X-ray sources and television use heat to excite electrons into vacuum.[1] However, such cathodes are unstable when their dimensions approach a micro size. Therefore, cold cathode electron field emitters are desirable for FE displays and other vacuum microelectronic devices.[2] Since the first study of the field emission (FE) of carbon nanotubes (CNTs) in 1995 by W. A. de Heer and coworkers,[3] the FE of carbon materials such as amorphous carbon,[4] diamond,[5–7] carbon nanofibers,[8] graphite,[9] and carbon films[10] has gained considerable interest and been intensively investigated. Among these, CNTs[11,12] have shown excellent FE properties owing to their large aspect ratio, excellent electrical conductivity, high thermal conductivity, and good mechanical properties.

Nevertheless, the most recently discovered graphene by Geim and Novoselov in 2004[13] appears to be more attractive for field electron emission applications, benefiting from its unique sharp edge structures. Various kinds of graphene forms such as graphene oxide sheets,[14] graphene films,[15,16] single layer graphene,[17] graphene nanoflakes,[18,19] and vertical standing graphene[20] have been studied in terms of their FE properties. The mechanisms of graphite nanostructures for FE have also been investigated theoretically.[21] Among these, the vertical standing graphene possessing high density of individual FE sites on the exposed atomic thin edges seems superior for FE applications as compared to graphene films with the graphene sheets lying on a substrate. Exciting results based on the vertical standing graphene, with low threshold field, large field enhancement factor (β), and high emission current density[22,23] have been achieved. Our recent study also demonstrated excellent FE performance of quasi-free standing graphene strips fabricated by thermal decomposition of C-face SiC,[24] where a turn-on field 1.81 V/μm and a field enhancement factor $\beta = 17140$ ($\Phi = 4.3$ eV) were observed. A stable FE performance over 120 h accompanied. These results suggest the quasi-free standing graphene sheets grown on SiC substrate have potential as a high performance cold cathode FE source.

To explore and find novel performance of the quasi-free standing graphene sheets grown on other SiC substrates, the FE features of the quasi-free standing graphene sheets grown on nonpolar (10-10) and polar SiC (000-1) substrates (C-face) were studied and compared. It was found that the FE performance of the vertically aligned graphene sheets (VAGSs) grown on nonpolar SiC (10-10) substrate is superior to that of VAGSs grown on polar SiC (000-1) substrate. The details of FE properties of the two VAGSs are studied and discussed in this article.

The VAGSs grown on the nonpolar SiC (10-10) and polar SiC (000-1) substrates under the same growth conditions were labeled as sample A and sample B, respectively. The detailed structural characteristics of the VAGSs and their growth mechanisms are described and discussed elsewhere, together with the parameters associated with the growth of the VAGSs on the two SiC substrates. The as-grown VAGSs samples look gray–black and their surfaces are covered with a planar graphene layer (like a graphene cap) tens of nanometers thick. To get high density FE-active sites, the surface graphene layer must

*Project supported by the National Key Basic Research Program of China (Grant No. 2011CB932700) and the National Natural Science Foundation of China (Grant Nos. 51272279, 51072223, and 50972162).

†Corresponding author. E-mail: lwguo@iphy.ac.cn

© 2013 Chinese Physical Society and IOP Publishing Ltd

be removed to expose the sharp edges of the VAGSs as active FE sites. Here oxygen plasma treatment for 8 mins on the sample surface was adopted to remove the top flat graphene layer, instead of heating the samples in air at 500 °C as reported in our earlier paper.[20] The oxygen plasma treatment has been confirmed to be an efficient way to improve the FE properties of CNTs by increasing the effective number of defects presented in their structures.[25]

The morphology of the prepared VAGSs samples was analyzed by using a scanning electron microscope (SEM, HITACHI S-4300) operated at an acceleration voltage of 10 kV. The structural quality of the VAGSs was analyzed using a high resolution Raman spectrometer (HORIBA Jobin Yvon, HR800) with a 532-nm laser excitation focused to a spot of about 1 μm in diameter. The FE characteristics of the VAGSs were measured in a ball-type chamber with a base pressure of $\sim 2 \times 10^{-7}$ Pa, as schematically shown in Fig. 1. The anode is a cylinder-shaped stainless steel probe with a diameter of 1 mm, and the sample was pasted onto a stainless steel stage with conductive glue as the cathode. In the FE measurements, the distance between the anode and the sample surface was kept 300 μm. The emission currents under different applied voltages were recorded by a custom-made *I*–*V* measurement system, where the bias was supplied by a power source Keithley248 and the emission current was measured by a Keithley 6514 electrometer. The samples were subjected to multiple cycles of voltage sweeping until a stable emission obtained. The emission currents and applied voltages were recorded automatically by a computer program.

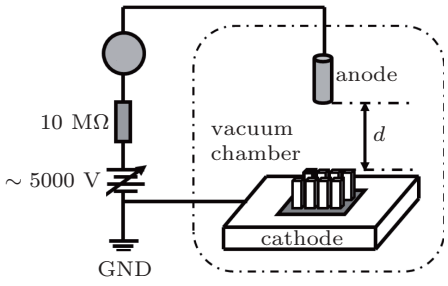


Fig. 1. Schematic plot of the electron emission measurement system.

Figures 2(a) and 2(b) show the top view images of samples A and B after oxygen plasma treatment. It is observed that the surface morphologies of the two samples are clearly different. For sample A as shown in Fig. 2(a), most of the basal planes of the VAGSs are parallel to each other, showing a unidirectional alignment. The ordering alignment of the VAGSs will generate space ordered electron emission facilitating realization of line scan display functions. While for sample B as shown in Fig. 2(b), the crystalline planes of the VAGSs show a petaloid-shaped arrangement, whose arrangement in space is random and dense compared with that of the sample A. In other words, the density of VAGSs on sample B is a little larger than that of the sample A. Besides the morphology characteristics, crystalline qualities of the VAGSs were analyzed by Raman scattering as shown in Fig. 2(c). The Raman spectra show three main peaks located around 1350, 1582, and 2700 cm^{-1}, attributed to *D*, *G*, and 2*D* peaks respectively, which are typical fingerprints of free graphene. The *D* band arises due to defects like corrugation, twisting and edges.[26] It is noted the *D* peak was prominent in both the samples. This suggests that a number of defects or edges exist in the samples, which favors the electron emission from the defect or edge sites as reported in Ref. [22].

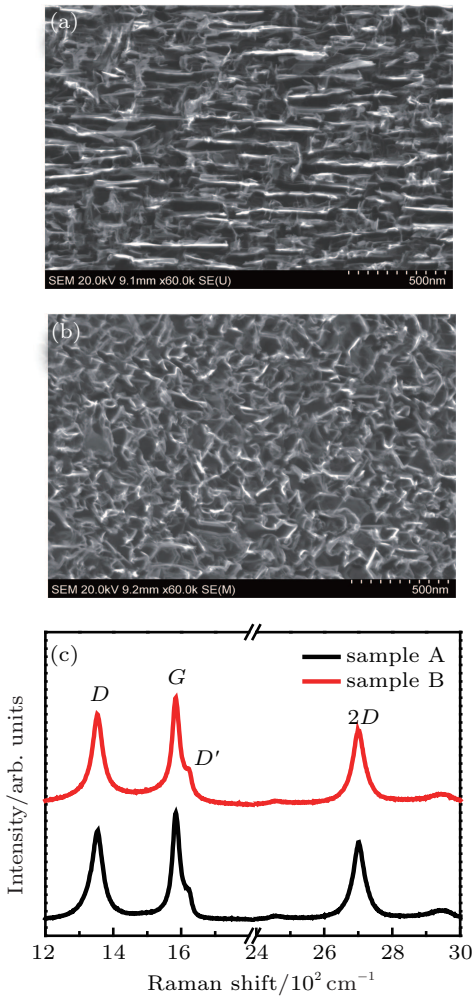


Fig. 2. (color online) (a) and (b) Top view SEM images of the sample A and sample B, where scale bar is 300 nm. (c) Normalized Raman scattering spectra of sample A (black curve) and sample B (red curve).

Figure 3(a) shows the FE features of the two samples. The current densities (*J*) as a function of applied electric field (*F*) are shown. The *J*–*F* plots demonstrate that the emission current density from sample A is higher relative to that from the sample B for a given applied field, which can be seen clearly from the left-shift of the plot from the sample A relative to that of the sample B. It is noted that the turn-on field of the sample A is about 4.6 V/μm which is a little lower than that of the

5.9 V/μm of the sample B, where the turn-on field (E_{to}) is defined as a field to produce a current density of 10 μA/cm^2. The higher turn-on field from the sample B may arise from either of two possible causes. One is the slightly curved top edges of the sample B induced by strong oxygen plasma treatment on the graphene sheets which are a little thinner than those of sample A. Another is the electrostatic screen effect provoked by nearby VAGSs due to its higher density with more emission sites compared with that of sample A. The electrostatic screen lowers the overall field enhancement of the emitter and leads to a higher turn-on field and smaller field enhancement in FE performance.[23] The effect had been observed and well explained in the FE of a high density CNT.[23] In addition, it should be explained that the higher turn-on field observed in our current samples compared with our early results[20] is due to the different top edge shapes of the graphene sheets. The edge shapes are determined by the different surface modification procedure used to remove the top flat graphene layer capped on the surface of the VAGSs. The edge shapes have a close relation to the effective emission sites and local electric field distribution, which directly determine the FE features. Therefore, developing a simple and reproducible surface modification procedure is among our plans to improve the FE performance of the VAGSs.

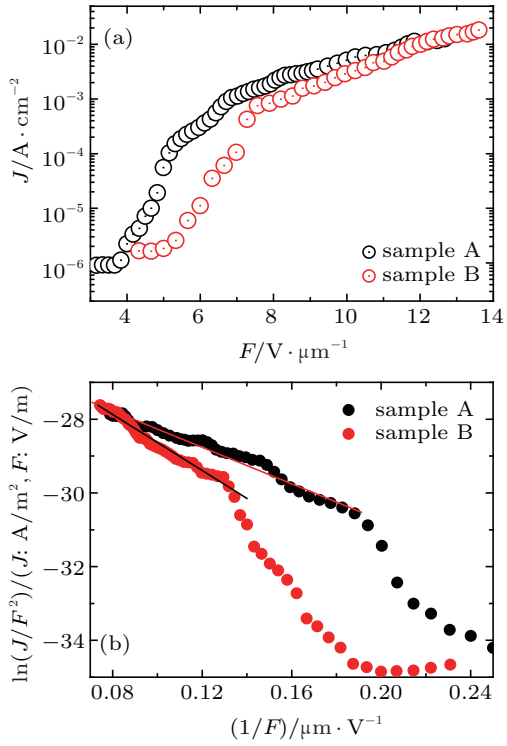


Fig. 3. (color online) (a) Typical plots of the electron emission current density (J) as a function of applied electric field. (b) The corresponding Fowler–Nordheim plots. The black (red) symbol is for sample A (B).

As is well known, the Fowler–Nordheim theory is the most commonly used model for describing the cold electron emission from a metal under a strong applied field.[27] The FE characteristics can be described by the Fowler–Nordheim equation: $J = (A\beta^2F^2/\Phi)\exp(-B\Phi^{3/2}/\beta F)$, where A and B are constants equal to 1.54×10^{-10} A/V^2·eV and 6.83×10^9 V/(eV)$^{3/2}$·m^{-1}, Φ is the work function of the emitter and β is the geometrical field enhancement factor of the emitter. We assume that the work function of our graphene samples is the same as that of graphite ($\Phi \approx 5$ eV). The field enhancement factor β can be deduced from the slope of the curves plotted as ln (J/F^2) versus $1/F$ at high field, as shown in Fig. 3(b). The field enhancement factors were estimated to be about 3165 and 1931 for the samples A and B, respectively. The large field enhancement factor from the VAGSs on the nonpolar SiC (10-10) substrate allows for sufficient tunneling of electrons through vacuum barriers, which is consistent with the lower turn-on field observed in the sample A as shown above. Meanwhile, it is noted that the F–N plot is composed of two near-linear regions in fields higher than the turn-on fields as shown in Fig. 3(b). The slope in the low field region is steeper than that in the high field region, as is often observed in carbon-based materials.[28,29] A slope decrease in the high field region has been well described in theory[30] based on space charge accumulation near the emitter, which sufficiently alters the cathode electric field.

In addition, FE stability is also an important parameter for checking the reliability of the VAGSs as a cold electron emission source. To evaluate the FE stability of the samples, time-dependent emission current was recorded over 8 hours as shown in Fig. 4. The maximum current fluctuation is around 7% for the sample A, whereas it reduces to only 4% for the sample B, which suggests the sample B has a slightly better FE stability. The observed emission stability of both are comparable to the reported results.[20] The better emission stability of sample B may be due to the disorder-linked distribution of the VAGSs, which renders stable emitting sites on the surface. Also, the disorder-linked arrangement of the VAGSs enables better heat dissipation, which decreases the Joule heating effect and protects the emission sites effectively.

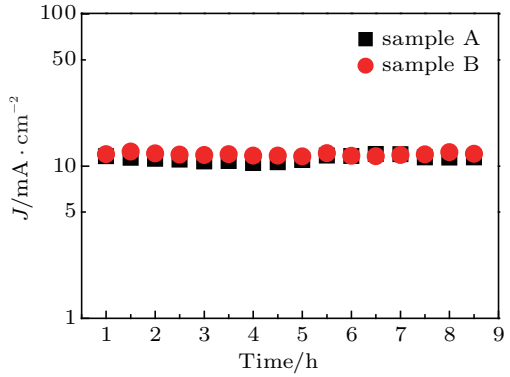


Fig. 4. (color online) FE stability experiments over 8 hours for sample A (black symbols) and sample B (red symbols).

In summary, the FE properties of VAGSs grown on nonpolar (10-10) and polar (000-1) SiC substrates were investigated and compared. It is found that the VAGSs grown on nonpolar SiC (10-10) substrate show unidirectional alignment and present better FE properties with a slightly lower turn-on field and a large field enhancement factor. The VAGSs grown on polar SiC (000-1) substrate behave better emission stability, which is important for undisrupted operation of an emitter. The better emission stability of the VAGSs grown on the polar SiC (000-1) substrate is attributed to the random-linked distribution of the VAGSs. If a simple and effective method for graphene edge modification is explored, the FE performance of the VAGSs will be enhanced significantly.

References

[1] Modinos A 1984 *Field, Thermionic and Secondary Electron Emission Spectroscopy* (New York: Plenum Press)
[2] Brodie I and Spindt C A 1992 *Advances in Electronics and Electron Physics* **83** 1
[3] Deheer W A, Chatelain A and Ugarte D 1995 *Science* **270** 1179
[4] Amaratunga G A J and Silva S R P 1996 *Appl. Phys. Lett.* **68** 2529
[5] Okano K, Koizumi S, Silva S R P and Amaratunga G A J 1996 *Nature* **381** 140
[6] Shang N G, Papakonstantinou P, Wang P, Zakharov A, Palnitkar U, Lin I N, Chu M and Stamboulis A 2009 *Acs Nano* **3** 1032
[7] Yang Y N, Zhang Z Y, Zhang F C, Dong J T, Zhao W, Zhai C X and Zhang W H 2012 *Chin. Phys. Lett.* **29** 018103
[8] Teng I J, Hsu H L, Jian S R, Kuo C T and Juang J Y 2012 *Nanoscale* **4** 7362
[9] Wang S M, Tian H W, Meng Q N, Zhao C M, Qiao L, Bing Y F, Hu C Q, Zheng W T and Liu Y C 2012 *Appl. Surf. Sci.* **258** 6930
[10] Wang Y Y, Li Y A, Xu J S and Gu G R 2012 *Chin. Phys. B* **21** 087902
[11] Lee D H, Kim J E, Han T H, Hwang J W, Jeon S, Choi S Y, Hong S H, Lee W J, Ruoff R S and Kim S O 2010 *Adv. Mater.* **22** 1247
[12] Zheng L W, Hu L Q, Xiao X J, Yang F, Lin H and Guo T L 2011 *Chin. Phys. B* **20** 128502
[13] Novoselov K S, Geim A K, Morozov S V, Jiang D, Zhang Y, Dubonos S V, Grigorieva I V and Firsov A A 2004 *Science* **306** 666
[14] Ye D X, Moussa S, Ferguson J D, Baski A A and El-Shall M S 2012 *Nano Lett.* **12** 1265
[15] Wu Z S, Pei S F, Ren W C, Tang D M, Gao L B, Liu B L, Li F, Liu C and Cheng H M 2009 *Adv. Mater.* **21** 1756
[16] Wang X P, Liu X F, Liu X X, Wang L J, Yang C, Jing L W, Li S K and Pan X F 2012 *Chin. Phys. B* **21** 128102
[17] Xiao Z M, She J C, Deng S Z, Tang Z K, Li Z B, Lu J M and Xu N S 2010 *Acs Nano* **4** 6332
[18] Li L, Sun W N, Tian S B, Xia X X, Li J J and Gu C Z 2012 *Nanoscale* **4** 6383
[19] Soin N, Roy S S, Roy S, Hazra K S, Misra D S, Lim T H, Hetherington C J and McLaughlin J A 2011 *J. Phys. Chem. C* **115** 5366
[20] Jiang L L, Yang T Z, Liu F, Dong J, Yao Z H, Shen C M, Deng S Z, Xu N S, Liu Y Q and Gao H J 2013 *Adv. Mater.* **25** 250
[21] Araidai M, Nakamura Y and Watanabe K 2004 *Phys. Rev. B* **70** 245410
[22] Koh A T T, Foong Y M, Pan L K, Sun Z and Chua D H C 2012 *Appl. Phys. Lett.* **101** 183107
[23] Malesevic A, Kemps R, Vanhulsel A, Chowdhury M P, Volodin A and Van Haesendonck C 2008 *J. Appl. Phys.* **104** 084301
[24] Huang Q S, Wang G, Guo L W, Jia Y P, Lin J J, Li K, Wang W J and Chen X L 2011 *Small* **7** 450
[25] Wang Y Y, Gupta S, Liang M and Nemanich R J 2005 *J. Appl. Phys.* **97** 104309
[26] Malard L M, Pimenta M A, Dresselhaus G and Dresselhaus M S 2009 *Phys. Rep.* **473** 51
[27] Fowler R H and Nordheim L 1928 *Royal Soc. Lond. Proc.* **119** 173
[28] Ducati C, Barborini E, Piseri P, Milani P and Robertson J 2002 *J. Appl. Phys.* **92** 5482
[29] Lee K, Lim S C, Choi Y C and Lee Y H 2008 *Appl. Phys. Lett.* **93** 063101
[30] Barbour J P, Dolan W W, Trolan J K, Martin E E and Dyke W P 1953 *Phys. Rev.* **92** 45